ATP-EMTP study of current differential protection with synchronization and fault location functions

M. M. Saha, J. Izykowski, E. Rosolowski

***Abstract*--This paper considers fault location and analytical synchronization of two-end measurements functions as embedded into a current differential protective relay. As a result of that, incomplete two-end measurements, i.e. three-phase currents measured at both line ends, while three-phase voltage only from only one end are considered for processing. Fault location and synchronization formulae are derived with considering a distributed-parameter model of a transposed overhead power line. The performed ATP-EMTP based evaluation proved the validity of the presented algorithms and their high accuracy.**

***Keywords*: ATP-EMTP, transmission line, fault simulation, current differential protection, synchronization of two-end measurements, fault location.**

I. Preparation of the Final Manuscript

AMONG different concepts which are utilized in protective relaying of power systems, a unit protection is considered as the most efficient one. Such the concept results in individual protection of sections of a power system. A current differential relay [1]–[5] appears as the unit protection system which is the most frequently used. Its principle is to sense the difference between the incoming and outgoing terminal currents of the protected section. This method is utilized for protecting power transformers, generators, generator-transformer units, motors, bus-bars and power lines.

The considerations of this paper are focused on increasing the functionality of a current differential relay designated for protecting long overhead transmission lines (Fig. 1), i.e. in equipping a relay with the following functions:

- synchronization of two-end measurements [4],
- fault location for an inspection-repair purpose [6].

Power transmission lines are distinctive from the other power system components by their longitudinal size. Because of long distances between the line terminals the extra media for information interexchange is required and sophisticated methods of two-end measurement data alignment are applied.

M. M. Saha is with ABB AB, Department of Research & Development, SE-721 59 Västerås, Sweden (e-mail: murari.saha@se.abb.com).

J. Izykowski is with Wroclaw University of Technology, Wroclaw, Poland (e-mail: jan.izykowski@pwr.wroc.pl).

E. Rosolowski is with Wroclaw University of Technology, Wroclaw, Poland (e-mail: eugeniusz.rosolowski@pwr.wroc.pl).

Paper submitted to the International Conference on Power Systems Transients (IPST2013) in Vancouver, Canada June 18-20, 2013.

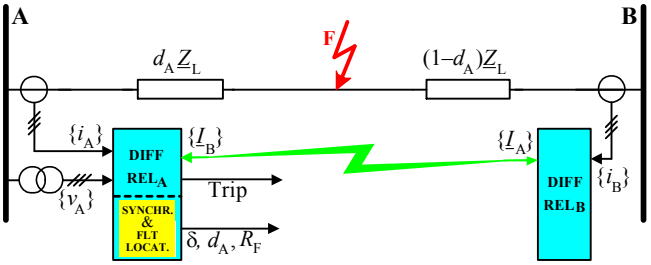

Fig. 1. Functions of synchronization of two-end measurements (SYNCHR.) and fault location (FLT LOCAT.) embedded into current differential relay

One of the most effective solutions is a 'ping-pong' algorithm [1]. The transmitted data are stamped locally with time tags which allow for estimation of actual delay in both directions even in case of channel propagation time asymmetry. The most precise method of delay compensation and sampling synchronization is based on the satellite Global Positioning System (GPS) [2]–[3]. However, reliance on the system independent of the protection system owner is not optimal solution. Therefore, in this paper a fault location function is considered as performed with utilizing two-end unsynchronized measurements. This is substantial difference in comparison to the earlier approach presented in [5] where the considerations were carried out under an assumption that the measurements are perfectly synchronized.

This paper presents the new algorithm for locating faults on two-terminal power transmission line. It is assumed here (Fig. 1) that the fault locator (FLT LOCAT.) is embedded into the current differential relay from the terminal A. Besides the phasors of three-phase currents (of phases: a, b, c – as denoted in the subscripts) from the end A: $\{\underline{I}_A\}=\{\underline{I}_{Aa}, \underline{I}_{Ab}, \underline{I}_{Ac}\}$ and from the end B: $\{\underline{I}_B\}=\{\underline{I}_{Ba}, \underline{I}_{Bb}, \underline{I}_{Bc}\}$, which are utilized for a protection purpose, the fault locator is additionally supplied with three-phase voltage $\{v_A\}=\{v_{Aa}, v_{Ab}, v_{Ac}\}$ from the local line end (A). Thus, the fault locator is designed as utilizing the communication infrastructure of the current differential relays, thus not demanding additional communication links. As a result, a current differential relay besides its main feature, i.e. indicating whether a fault occurred within a line or outside it (the protection duty), also provides information on accurate position of the fault, which is required for an inspection-repair purpose [6].

With the aim of providing high accuracy for locating faults on long lines, the distributed-parameter line model (Fig. 2) is strictly utilized in the presented algorithms. Both, the voltage drop across the faulted line segment and also across the fault

path resistance are determined with strict consideration of the distributed parameter line model. The respective line model for a general *i*-th symmetrical component is shown in Fig. 2.

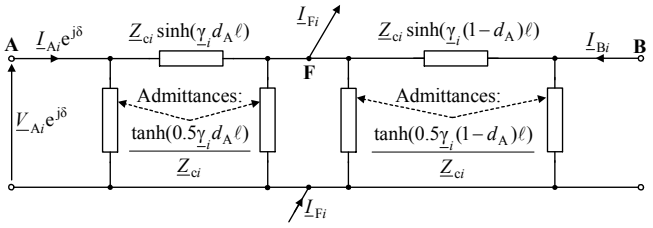

Fig. 2. Distributed-parameter model of faulted line for the *i*-th symmetrical components sequence

In this paper, use of incomplete two-end unsynchronized measurements [6] is considered. Due to insufficient measurement data, instead of processing the signals of the individual symmetrical components, the natural fault loops are to be considered. Accordingly to the identified fault type, the single phase loop (for phase-to-ground faults) and inter-phase loop (for faults involving two or three phases) have to be considered. The fault loop contains the section of the line from the measuring point (A) up to the fault point (F) and the fault path resistance.

The paper starts with derivation of the fault location algorithm. Then, the results for the example fault, using the signals from ATP-EMTP simulation [7], are presented and discussed.

II. Fault Location Algorithm

The fault location algorithm is derived utilizing a generalized fault loop model [6] which allows to describe the considered fault loop using a single formula involving the coefficients dependent on fault type.

A. Generalized fault loop model

The generalized fault loop model [6], which in the considered case describes the fault loop seen from the line end A (where the fault locator is considered as embedded into the current differential relay) is stated as follows:

$$\underline{V}_{\mathrm{Fp}}(d_{\mathrm{A}}) - R_{\mathrm{F}}\underline{I}_{\mathrm{F}} = 0 \tag{1}$$

where:

$\underline{V}_{\mathrm{Fp}}(d_{\mathrm{A}})$ – fault loop voltage composed accordingly to the fault type, obtained after its analytic transfer from the fault locator installation point (the bus A) to the fault point F,

d_{A} – unknown relative distance to fault (p.u.),

R_{F} – fault path resistance,

$\underline{I}_{\mathrm{F}}$ – total fault current (fault path current).

B. Fault loop voltage at fault point

Transfer of the original fault loop voltage from the bus A to the fault point F can be represented with use of a weighted sum of the respective symmetrical components:

$$\underline{V}_{\mathrm{Fp}}(d_{\mathrm{A}}) = \underline{a}_1\underline{V}_{\mathrm{F1}} + \underline{a}_2\underline{V}_{\mathrm{F2}} + \underline{a}_0\underline{V}_{\mathrm{F0}} \tag{2}$$

where: subscripts denoting the component type are as follows:
1 – positive-, 2 – negative-, 0 – zero-sequence,

$\underline{a}_1$, $\underline{a}_2$, $\underline{a}_0$ – weighting coefficients dependent on fault type [6], as gathered in Table I.

TABLE I.
WEIGHTING COEFFICIENTS FOR COMPOSING FAULT LOOP VOLTAGE (2)

Fault Type	$\underline{a}_1$	$\underline{a}_2$	$\underline{a}_0$
a–g	1	1	1
b–g	$\underline{a}^2$	$\underline{a}$	1
c–g	$\underline{a}$	$\underline{a}^2$	1
a–b, a–b–g a–b–c, a–b–c–g	$1-\underline{a}^2$	$1-\underline{a}$	0
b–c, b–c–g	$\underline{a}^2-\underline{a}$	$\underline{a}-\underline{a}^2$	0
c–a, c–a–g	$\underline{a}-1$	$\underline{a}^2-1$	0
$\underline{a}=\exp(\mathrm{j}2\pi/3)$; $\mathrm{j}=\sqrt{-1}$			

Applying the distributed-parameter line model [6], the symmetrical components of voltages from (2) are determined as follows:

$$\underline{V}_{\mathrm{F1}} = [\underline{V}_{\mathrm{A1}}\cosh(\underline{\gamma}_1\ell d_{\mathrm{A}}) - \underline{Z}_{\mathrm{c1}}\underline{I}_{\mathrm{A1}}\sinh(\underline{\gamma}_1\ell d_{\mathrm{A}})]\mathrm{e}^{\mathrm{j}\delta} \tag{3}$$

$$\underline{V}_{\mathrm{F2}} = [\underline{V}_{\mathrm{A2}}\cosh(\underline{\gamma}_1\ell d_{\mathrm{A}}) - \underline{Z}_{\mathrm{c1}}\underline{I}_{\mathrm{A2}}\sinh(\underline{\gamma}_1\ell d_{\mathrm{A}})]\mathrm{e}^{\mathrm{j}\delta} \tag{4}$$

$$\underline{V}_{\mathrm{F0}} = [\underline{V}_{\mathrm{A0}}\cosh(\underline{\gamma}_0\ell d_{\mathrm{A}}) - \underline{Z}_{\mathrm{c0}}\underline{I}_{\mathrm{A0}}\sinh(\underline{\gamma}_0\ell d_{\mathrm{A}})]\mathrm{e}^{\mathrm{j}\delta} \tag{5}$$

where:

$\mathrm{e}^{\mathrm{j}\delta}$ – synchronization operator (δ – unknown synchronization angle) ensuring common time base of digital measurements from the buses A and B,

$\underline{V}_{\mathrm{A1}}$, $\underline{V}_{\mathrm{A2}}$, $\underline{V}_{\mathrm{A0}}$ – symmetrical components of side A voltages,

$\underline{I}_{\mathrm{A1}}$, $\underline{I}_{\mathrm{A2}}$, $\underline{I}_{\mathrm{A0}}$ – symmetrical components of side A currents,

ℓ – length of the line (km),

$\underline{\gamma}_1 = \sqrt{\underline{Z}'_{\mathrm{1L}}\underline{Y}'_{\mathrm{1L}}}$ – propagation constant of the line for the positive- (negative-) sequence,

$\underline{\gamma}_0 = \sqrt{\underline{Z}'_{\mathrm{0L}}\underline{Y}'_{\mathrm{0L}}}$ – propagation constant of the line for the zero-sequence,

$\underline{Z}_{\mathrm{c1}} = \sqrt{\underline{Z}'_{\mathrm{1L}}/\underline{Y}'_{\mathrm{1L}}}$ – characteristic impedance of the line for the positive-sequence (negative-sequence),

$\underline{Z}_{\mathrm{c0}} = \sqrt{\underline{Z}'_{\mathrm{0L}}/\underline{Y}'_{\mathrm{0L}}}$ – characteristic impedance of the line for the zero-sequence,

$\underline{Z}'_{\mathrm{1L}} = R'_{\mathrm{1L}} + \mathrm{j}\omega_1 L'_{\mathrm{1L}}$ – impedance of the line for the positive-sequence (negative-sequence) (Ω/km),

$\underline{Z}'_{\mathrm{0L}} = R'_{\mathrm{0L}} + \mathrm{j}\omega_1 L'_{\mathrm{0L}}$ – impedance of the line for the zero-sequence (Ω/km),

$\underline{Y}'_{\mathrm{1L}} = G'_{\mathrm{1L}} + \mathrm{j}\omega_1 C'_{\mathrm{1L}}$ – admittance of the line for the positive-sequence (negative-sequence) (S/km),

$\underline{Y}'_{\mathrm{0L}} = G'_{\mathrm{0L}} + \mathrm{j}\omega_1 C'_{\mathrm{0L}}$ – admittance of the line for the zero-

sequence (S/km),

R'_{1L}, L'_{1L}, G'_{1L}, C'_{1L} – resistance, inductance, conductance and capacitance of the line for the positive-sequence (negative-sequence) per km length,

R'_{0L}, L'_{0L}, G'_{0L}, C'_{0L} – resistance, inductance, conductance and capacitance of the line for the zero-sequence per km length.

The line parameters for the positive- and negative-sequences are identical and therefore they are uniformly denoted with '1' in the subscripts for both sequences.

C. Total fault current

Adding phase currents (from phases: a, b, c) from both line ends (A and B) appears as the simplest way of determining the fault current in particular phases at the fault point. However, this way reveals as affected by the currents charging line shunt capacitances. This is so, since in the currents summed are lessen by the currents charging line shunt capacitances. This is the explanation why the natural way of determining the total fault current is not used here. Instead, the detailed analysis of the flow of currents in the faulted line is considered.

Taking into account the share of individual symmetrical components of the total fault current (denoted with the respective subscripts: 1 – positive-, 2 – negative-, 0 – zero-sequence, respectively): $\underline{I}_{F1}$, $\underline{I}_{F2}$, $\underline{I}_{F0}$, one obtains [5]–[6]:

$$\underline{I}_F = \underline{a}_{F1}\underline{I}_{F1} + \underline{a}_{F2}\underline{I}_{F2} + \underline{a}_{F0}\underline{I}_{F0} \tag{6}$$

where:

$\underline{a}_{F1}$, $\underline{a}_{F2}$, $\underline{a}_{F0}$ – share coefficients, dependent on fault type and the assumed preference with respect to using particular sequences (the recommended set is delivered in Table II).

TABLE II
SHARE COEFFICIENTS FOR COMPOSING TOTAL FAULT CURRENT (6)

Fault Type	$\underline{a}_{F1}$	$\underline{a}_{F2}$	$\underline{a}_{F0}$
a–g	0	3	0
b–g	0	$3\underline{a}$	0
c–g	0	$3\underline{a}^2$	0
a–b	0	$1-\underline{a}$	0
b–c	0	$\underline{a}-\underline{a}^2$	0
c–a	0	$\underline{a}^2-1$	0
a–b–g	$1-\underline{a}^2$	$1-\underline{a}$	0
b–c–g	$\underline{a}^2-\underline{a}$	$\underline{a}-\underline{a}^2$	0
c–a–g	$\underline{a}-1$	$\underline{a}^2-1$	0
a–b–c, a–b–c–g	$1-\underline{a}^2$	$1-\underline{a}$ *)	0
*) – there is no negative sequence component under these faults and the coefficient can be assumed as equal to zero			

There is a possibility of applying different, alternative sets of the share coefficients [5]–[6], however, the coefficients for which the zero-sequence is eliminated ($\underline{a}_{F0}=0$) – as in Table 2, is recommended for the considered fault location algorithm. In this way, use of the line parameters for the zero-sequence – which are considered as unreliable data, is avoided for determining the total fault current. This is advantageous for assuring the highest possible accuracy of fault location.

This is important that for the share coefficients proposed in Table II the preference of using the negative-sequence over the positive-sequence is set for single-phase and phase-to-phase faults.

Accurate determination of the symmetrical components of the total fault current can be performed with strict consideration of the distributed-parameter model of the faulted line (Fig. 2). Taking this model into the consideration, one derives the following formula for the *i*-th symmetrical component of the total fault current [6]:

$$\underline{I}_{Fi} = \frac{\underline{M}_i(e^{j\delta})}{\underline{Z}_{ci}\cosh(\underline{\gamma}_i\ell(1-d_A))} \tag{7}$$

where:

$$\underline{M}_i(e^{j\delta}) = \underline{Z}_{ci}\underline{I}_{Bi} + \underline{N}_{Ai}e^{j\delta}$$

$$\underline{N}_{Ai} = \underline{Z}_{ci}\underline{I}_{Ai}\cosh(\underline{\gamma}_i\ell) - \underline{V}_{Ai}\sinh(\underline{\gamma}_i\ell)$$

i=1: positive-sequence, *i*=2: negative-sequence and: *i*=0: zero-sequence.

The obtained formula (7) for the *i*-th symmetrical component of the total fault current is compact and the unknown distance to fault (d_A) is involved in the denominator, while the synchronisation operator (exp(jδ)) in the nominator of (7) only.

Substituting the positive- and negative-sequence components of the total fault current, determined in (7), into (6), and also taking into account that the zero-sequence is eliminated (Table II), one obtains the total fault current in the form:

$$\underline{I}_F = \frac{\underline{a}_{F1}\underline{M}_1(e^{j\delta}) + \underline{a}_{F2}\underline{M}_2(e^{j\delta})}{\underline{Z}_{c1}\cosh(\underline{\gamma}_1\ell(1-d_A))} \tag{8}$$

Substitution of the total fault current (8) into the generalized fault loop model (1) yields:

$$\underline{V}_{Fp}(d_A) - R_F\frac{\underline{a}_{F1}\underline{M}_1(e^{j\delta}) + \underline{a}_{F2}\underline{M}_2(e^{j\delta})}{\underline{Z}_{c1}\cosh(\underline{\gamma}_1\ell(1-d_A))} = 0 \tag{9}$$

where:

$\underline{V}_{Fp}(d_A)$ – defined in (2)–(5), with use of the weighting coefficients specified for different faults in Table I,

$\underline{M}_1(e^{j\delta})$, $\underline{M}_2(e^{j\delta})$ – quantities defined in (7),

$\underline{a}_{F1}$, $\underline{a}_{F2}$ – share coefficients dependent on the fault type, as gathered in Table II.

The derived fault location formula (9) is compact and covers different fault types, what requires setting the appropriate fault type coefficients, as provided in Table I and Table II.

There are three unknowns in the fault location formula (9): distance to fault (d_A), fault resistance (R_F) and synchronization

angle (δ). In order to cope with solution for such number of unknowns, additional equation involving the synchronization angle has to be formulated. For this purpose the boundary conditions of different fault types and also the analysis of pre-fault state have been considered.

Excluding the zero sequence components ($\underline{a}_{F0}=0$ as in Table II), the total fault current is:

$$\underline{I}_F = \underline{a}_{F1}\underline{I}_{F1} + \underline{a}_{F2}\underline{I}_{F2} \tag{10}$$

Two recommended characteristic sets of the share coefficients for the considered here phase-to-ground and phase-to-phase faults are provided in Table III. The other sets can be determined as well. However, use of the sets from Table III will result in getting simple analytic solution for a sought synchronization angle (δ).

TABLE III
TWO SETS OF SHARE COEFFICIENTS FOR PHASE-TO-GROUND FAULTS AND PHASE-TO-PHASE FAULTS

Fault Type	I–SET		II–SET	
	$\underline{a}_{F1}^{I-SET}$	$\underline{a}_{F2}^{I-SET}$	$\underline{a}_{F1}^{II-SET}$	$\underline{a}_{F2}^{II-SET}$
a–g	0	3	3	0
b–g	0	$3\underline{a}$	$3\underline{a}^2$	0
c–g	0	$3\underline{a}^2$	$3\underline{a}$	0
a–b	0	$1-\underline{a}$	$1-\underline{a}^2$	0
b–c	0	$\underline{a}-\underline{a}^2$	$\underline{a}^2-\underline{a}$	0
c–a	0	$\underline{a}^2-1$	$\underline{a}-1$	0

Applying the sets from Table III the total fault current can be expressed as follows:

$$\underline{I}_F = \underline{a}_{F1}^{I-SET}\underline{I}_{F1} + \underline{a}_{F2}^{I-SET}\underline{I}_{F2} \tag{11}$$

or alternatively:

$$\underline{I}_F = \underline{a}_{F1}^{II-SET}\underline{I}_{F1} + \underline{a}_{F2}^{II-SET}\underline{I}_{F2} \tag{12}$$

Comparing (11) with (12) and taking into account (7) one gets the following formula for the synchronization operator for faults in Table III:

$$[e^{j\delta}]_{ph-g,\,ph-ph} = \frac{\underline{Z}_{c1}(\underline{a}_{F2}^{I-SET}\underline{I}_{B2} - \underline{a}_{F1}^{II-SET}\underline{I}_{B1})}{\underline{a}_{F1}^{II-SET}\underline{N}_{A1} - \underline{a}_{F2}^{I-SET}\underline{N}_{A2}} \tag{13}$$

In case of phase-to-phase-to-ground faults an analysis of the boundary conditions yields the following relation between the zero-, positive- and negative-sequence components of the total fault current [6]:

$$\underline{I}_{F0} = \underline{b}_{F1}\underline{I}_{F1} + \underline{b}_{F2}\underline{I}_{F2} \tag{14}$$

where:

$\underline{b}_{F1}$, $\underline{b}_{F2}$ – coefficients delivered in Table IV.

TABLE IV
COEFFICIENTS INVOLVED IN THE RELATION (14)

Fault Type	$\underline{b}_{F1}$	$\underline{b}_{F2}$
a–b–g	$-\underline{a}$	$-\underline{a}^2$
b–c–g	–1	–1
c–a–g	$-\underline{a}^2$	$-\underline{a}$

Substituting (7) into (14) results in:

$$\frac{\underline{Z}_{c0}\underline{I}_{B0} + \underline{N}_{A0}[e^{j\delta}]_{ph-ph-g}}{\underline{Z}_{c0}\cosh(\underline{\gamma}_0\ell(1-d_A))} = \frac{\underline{Z}_{c1}(\underline{b}_{F1}\underline{I}_{B1} + \underline{b}_{F2}\underline{I}_{B2}) + (\underline{b}_{F1}\underline{N}_{A1} + \underline{b}_{F2}\underline{N}_{A2})[e^{j\delta}]_{ph-ph-g}}{\underline{Z}_{c1}\cosh(\underline{\gamma}_1\ell(1-d_A))} \tag{15}$$

For three-phase balanced faults one can derive for the pre-fault state (superscript: pre) positive-sequence:

$$[e^{j\delta}]_{3ph} = \frac{-\underline{Z}_{c1}\underline{I}_{B1}^{pre}}{-\sinh(\underline{\gamma}_1\ell)\underline{V}_{A1}^{pre} + \underline{Z}_{c1}\cosh(\underline{\gamma}_1\ell)\underline{I}_{A1}^{pre}} \tag{16}$$

Distance to fault is not involved in determination of the synchronization operator (16).

After resolving (9) into the real and imaginary parts and taking the respective relation: (13) or (15) or (16), one of the known numeric procedures for solving nonlinear equations can be applied. It has been checked that the Newton-Raphson iterative method is a good choice for that.

III. ATP-EMTP BASED EVALUATION STUDY

Performance of the presented method was analysed using a digital model running on ATP-EMTP simulation software program [7]. A single-circuit transmission line was used in the simulation. The main parameters of the modeled transmission system were assumed as follows:

- rated voltage: 400kV
- line length: 300km
- system frequency: 50 Hz
- phase angle of EMFs of Systems: A: 0°, B: (–30°)
- sequence impedances of equivalent systems:
  $\underline{Z}_{1SA}=\underline{Z}_{1SB}=(1.307+j15)\Omega$,
  $\underline{Z}_{0SA}=\underline{Z}_{0SB}=(2.318+j26.5)\Omega$
- line impedances:
  $\underline{Z}_{1L}=(0.0267+j0.3151)\Omega$/km
  $\underline{Z}_{0L}=(0.275+j1.026)\Omega$/km
- line shunt capacitances:
  $C_{1L}=0.013\mu$F/km, $C_{0L}=0.0085\mu$F/km.

Different scenarios with changing of a fault were considered in the performed evaluation study. Fault type, fault resistance and equivalent system impedances were changed.

The two-end measurements obtained from the simulation were perfectly synchronized. Therefore, an intentional de-synchronization of the measurements was introduced.

In order to examine the errors of the presented fault location algorithm itself, the errorless transformation of instrument transformers (both for current and voltage) was assumed at the first stage of the evaluation. Then, the instrument transformers with typical parameters were included into the simulation model.

Analog low-pass filters with 350Hz cut-off frequency were also included. The sampling frequency of 1000Hz was applied and the respective phasors were determined with use of the DFT algorithm.

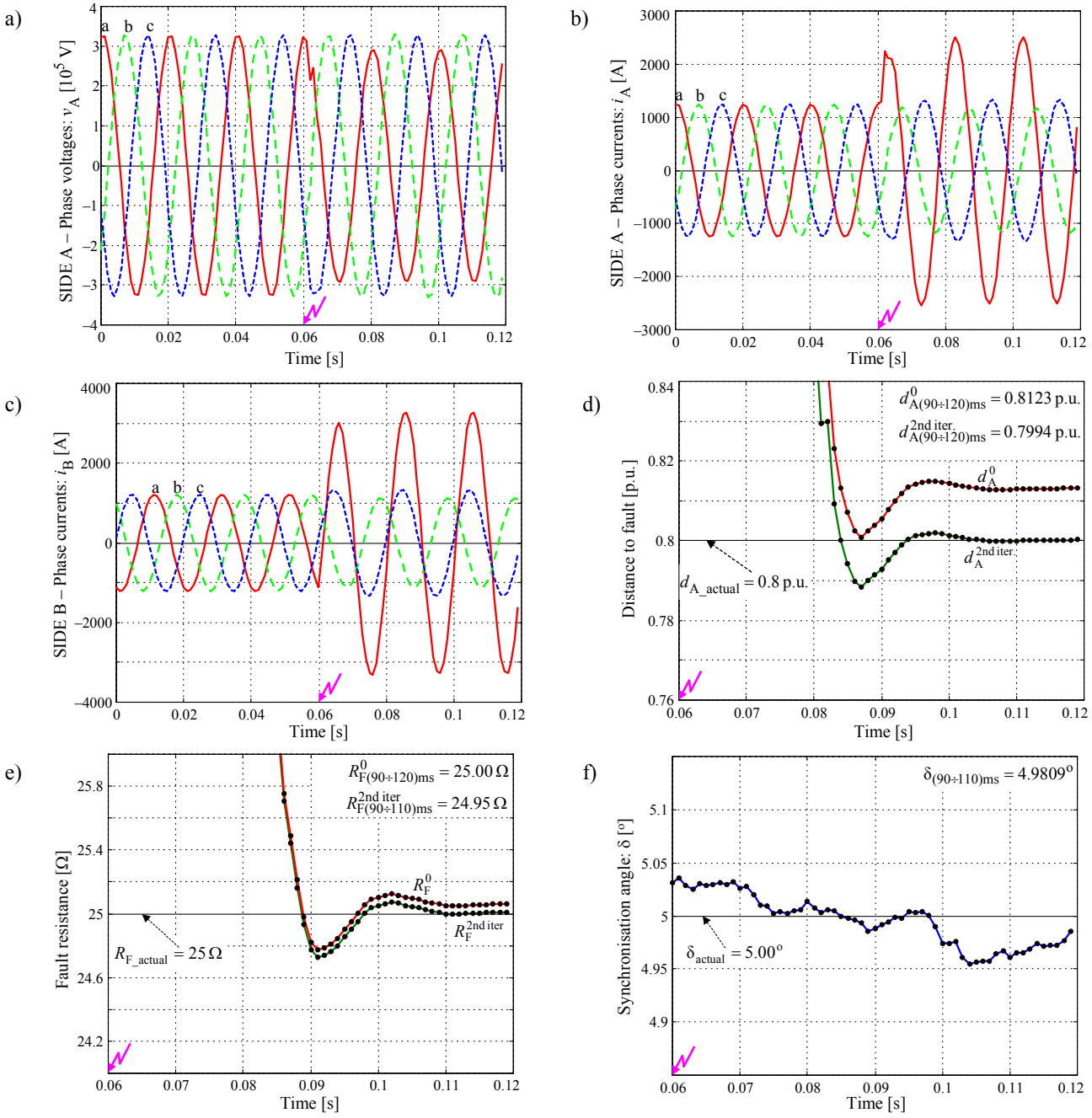

Fig. 3. The sample fault example: a) three-phase voltage of side A, b) three-phase current of side A, c) three-phase current of side B, d) calculated distance to fault, e) calculated fault resistance, f) calculated synchronization angle

The obtained results for the distance to fault, fault resistance and synchronization angle of all test cases were correct and accurate.

Fig. 3 presents the measured three-phase signals and the calculation results for the sample single phase a–g fault. The following specifications for this fault were taken: d_{A_actual}=0.8p.u., R_{F_actual}=25Ω, δ_{actual}=5°. The measurements from the bus A (both current and voltage) were intentionally delayed by 5° with respect to the measurement of the current from the remote line terminal (B).

In Fig. 3a–3c the three-phase measured signals are shown. For the applied comparatively high fault resistance (25Ω) there are no visible d.c. components in phase currents (they decay with a high speed). Distance to fault (Fig. 3d) and fault resistance (Fig. 3e) are obtained in iterative calculations. The start of these calculations (iteration number '0') was taken by transferring the equations to the form relevant for a lumped-parameter line model. This results in obtaining some errors in calculated results. As for example, the distance to fault averaged within the interval from 90 to 110ms (or from 30 to 50ms of the fault time since the fault was applied at t=60ms) : $d^0_{A(90\div110)ms} = 0.8123$ p.u. differs by around 1.2% from the actual result (0.8p.u.). However, after performing two

iterations (superscript: '2nd iter') very accurate result: $d^{\text{2nd iter}}_{\text{A(90÷110)ms}} = 0.7994$ p.u. is obtained. The synchronization angle determined for this fault type according to (13): δ=4.9802° is very close to the introduced de-synchronization angle (5.000°).

Different specifications of faults and pre-fault power flows have been considered in the evaluation of the accuracy of the developed fault location algorithm. For the faults involving fault resistance up to 25 Ω, the maximum errors do not exceed the following values for the case of the instrument transformers with ideal transformation:

- 2% – when applying the lumped-parameter line model (no iterative calculations).
- 0.2%. – when applying the distributed-parameter line model (after performing 2 iterations of the calculations).

The sample evaluation results (the distance to fault: d [p.u.] and the fault location error [%]) for a-g faults applied at different locations are presented in Table V (for fault resistance: 10Ω) and in Table VI (for fault resistance: 25Ω) confirm the above statement. The iterative calculations converge very fast and there is a very small difference between the results of the first and the second iterations.

TABLE V
FAULT LOCATION ACCURACY – a-g FAULT, R_F=10Ω

d_{exact}	Iteration: 0		Iteration: 1		Iteration: 2	
[p.u.]	d^0 [p.u.]	Err^0 [%]	d^1 [p.u.]	Err^1 [%]	d^2 [p.u.]	Err^2 [%]
0.1	0.09992	0.008228	0.09983	0.01685	0.09983	0.01685
0.2	0.1999	0.01367	0.1997	0.03393	0.1997	0.03394
0.3	0.3001	0.01495	0.2996	0.04201	0.2996	0.04205
0.4	0.4009	0.08803	0.3995	0.04771	0.3995	0.04791
0.5	0.5023	0.2315	0.4996	0.04271	0.4996	0.04331
0.6	0.6046	0.4628	0.5997	0.02825	0.5997	0.0297
0.7	0.7078	0.7804	0.6997	0.02528	0.6997	0.02829
0.8	0.8124	1.238	0.8	0.00466	0.7999	0.01027
0.9	0.9182	1.819	0.8999	0.01108	0.8998	0.0205

TABLE VI
FAULT LOCATION ACCURACY – a-g FAULT, R_F=25Ω

d_{exact}	Iteration: 0		Iteration: 1		Iteration: 2	
[p.u.]	d^0 [p.u.]	Err^0 [%]	d^1 [p.u.]	Err^1 [%]	d^2 [p.u.]	Err^2 [%]
0.1	0.1002	0.01803	0.09995	0.004643	0.09995	0.004616
0.2	0.2002	0.0197	0.1998	0.01905	0.1998	0.01903
0.3	0.3004	0.04134	0.2996	0.03802	0.2996	0.03803
0.4	0.4011	0.1108	0.3995	0.05093	0.3995	0.05105
0.5	0.5025	0.2459	0.4994	0.05806	0.4994	0.0585
0.6	0.6045	0.4543	0.5993	0.06939	0.5993	0.07054
0.7	0.7076	0.7637	0.6992	0.07856	0.6992	0.08103
0.8	0.8123	1.231	0.7995	0.05437	0.7994	0.059
0.9	0.9182	1.817	0.8994	0.06081	0.8993	0.06847

The fault location errors can be even reduced by applying more advanced filtration in place of the utilized DFT.

The other part of the evaluation study was conducted for the real instrument transformers included into the simulation model. In this case the fault location errors do not exceed 1.5% with applying iterative calculations for the distributed-parameter line model.

IV. CONCLUSIONS

A new fault location algorithm utilizing unsynchronized measurements of two-end currents and one-end voltage is presented. It has been assumed that such fault location algorithm is incorporated into the current differential relay. In this way, the communication between the line ends of differential relays is utilized. By embedding the fault location and analytic synchronization of measurements functions into a relay, an increase of the relay functionality is simply achieved.

Compact forms of the equations for fault location and synchronization angle determination have been obtained. They are valid for different fault types and this is reflected by setting the appropriate fault type coefficients. High accuracy of fault location is assured by strict considering of the distributed-parameter line model. The solution of the derived equations is obtained with the Newton-Raphson iterative calculations.

The carried out evaluation with use of the fault data obtained from versatile simulation of faults on the test transmission network with a single-circuit long transmission line has proved that the derived algorithms can be effectively applied for increasing the functionality of protective differential relays. The included fault example and the selected results of the quantitative evaluation illustrate very good performance of the presented algorithms.

V. REFERENCES

[1] B. Kasztenny, G. Benmouyal, H. J. Altuve, and N. Fischer, "Tutorial on operating characteristics of microprocessor-based multiterminal line current differential relays," in *Proc. 2011 of the 38th Annual Western Protective Relay Conference, Spokane, WA*, p. 30.

[2] I. Hall, P. G. Beaumont, G. P. Baber, I. Shuto, M. Saga, K. Okuno and H. Ito, "New line current differential relay using GPS synchronization," in *Proc. 2003 IEEE Bologna PowerTech Conference, 23–26.06.2003, Bologna, Italy*.

[3] H. Y. Li, E. P. Southern, P. A. Crossley, S. Potts, S. D. A. Pickering, B. R. J. Caunce and G. C. Weller, "A new type of differential feeder protection relay using the Global Positioning System for data synchronization," *IEEE Trans. on Power Delivery*, Vol. 12, Issue 3, July 1997, pp. 1090–1099.

[4] M. Lukowicz, "New method of data transmission delay estimation for feeder differential protection," *Present Problems of Power System Control*, Publisher of Wroclaw University of Technology, Wroclaw, Poland, 2011, pp. 97–107.

[5] E. Rosolowski, J. Izykowski and M. M. Saha, "Using of current differential protection signals for fault location on two-terminal line," *Przeglad Elektrotechniczny (Electrical Review)*, Nr 5, 2008, pp. 9–13.

[6] M. M. Saha, J. Izykowski and E. Rosolowski, *Fault location on power networks*, Springer-Verlag, London, Series: Power Systems, 2010.

[7] H. Dommel, *Electro-Magnetic Transients Program*, Bonneville Power Administration, Portland, OR, 1986.